

Templated-assembly of conducting antimony cluster wires

J G Partridge, S A Brown¹, A D F Dunbar, R Reichel,
M Kaufmann, C Siegert, S Scott and R J Blaikie

Nanostructure Engineering Science and Technology Group and the MacDiarmid Institute for Advanced Materials and Nanotechnology, University of Canterbury, Private Bag 4800, Christchurch 8020, New Zealand

E-mail: simon.brown@canterbury.ac.nz

Received 5 May 2004, in final form 28 July 2004

Published 13 August 2004

Online at stacks.iop.org/Nano/15/1382

doi:10.1088/0957-4484/15/9/045

Abstract

Wires with meso- and nanoscale widths have been fabricated using a novel assembly technique based on the deposition of Sb clusters on templated surfaces. The template elements are V-grooves etched into the surface of a Si wafer. It is demonstrated that the clusters bounce or slide to the apex of the V-grooves, without significant fragmentation, and that this motion is the underlying mechanism behind the formation of the wires. The flow rate of inert gas into the cluster growth chamber controls the average velocity of the clusters and the morphology and width of the wires. Sb cluster-assembled wires with lengths over 150 μm and widths down to 100 nm have been assembled from ~ 40 nm diameter Sb clusters. Electrical contacts to the wires have been achieved via lithographic alignment of NiCr/Au contacts to the V-grooves prior to deposition.

1. Introduction

Atomic clusters exhibit a range of useful electronic, chemical and magnetic properties [1, 2] and show great potential as building blocks for nanoscale electronic and photonic devices (see for example [3–7]), but in order to incorporate these nanoscale building blocks in useful devices, it is essential that suitably controllable self-assembly methods are developed. To date, self-assembly of cluster structures has relied on surface diffusion of clusters [8–11], or of atoms which aggregate to form clusters [12]. Chains resembling wires can be achieved through diffusion to the naturally occurring step-edges on graphite [9, 10], but since the position of these surface defects is random, the placement of the wires cannot be controlled. Several attempts have therefore been made to use diffusion in conjunction with surface patterning techniques to control cluster assembly. In one study, a regular array of cluster structures was created by diffusion to an array of focused ion beam engraved defects on a graphite substrate [13]. Clusters

have also been aligned along the edges of optical photoresist templates on Si [14] and SiO₂ [15] to form uncontacted wire-like chains. So far, contacting to cluster-assembled wires has only been achieved using a relatively complex electrodeposition/lift-off technique [12].

The cluster assembly method reported here employs passivated Si V-grooves as template elements; the momentum of the deposited clusters causes them to bounce or slide to the apex of the V-groove (i.e. the direction of motion is defined by the incident momentum of the cluster), where they assemble into a wire. Since diffusion (i.e. random motion) of the clusters is not an important factor, the assembly process is insensitive to surface defects. The utilization of standard lithographic techniques to form the V-groove ensures control over the position of the wire, and preformed lithographically defined electrical contacts ensure that the wire is self-contacting.

2. Experiment

Substrates were processed from a SiO₂ coated (layer thickness 120 nm) Si wafer. Slots were patterned in the SiO₂ layer using optical lithography and reactive ion etching. These slots were translated into V-grooves in the underlying Si by placing the

¹ Address for correspondence: Department of Physics and Astronomy, University of Canterbury, Private Bag 4800, Christchurch 8020, Canterbury, New Zealand.

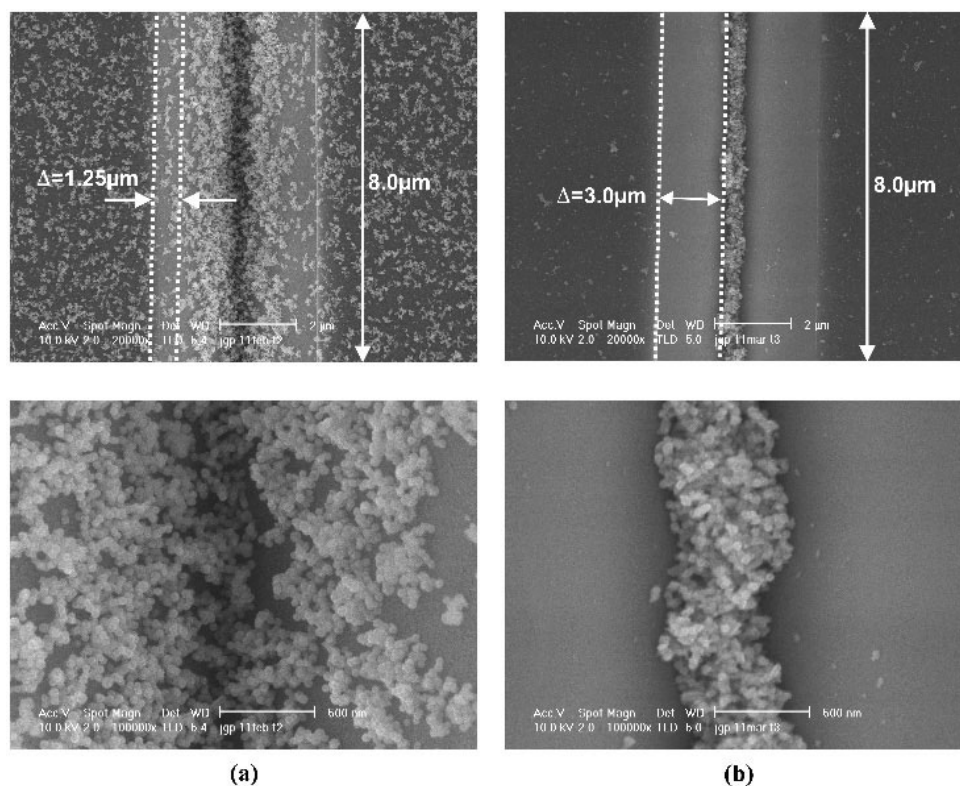


Figure 1. Low magnification (top) and high magnification (bottom) FE-SEM images of assembled Sb clusters deposited onto $4\ \mu\text{m}$ wide V-grooves deposited with source inlet Ar flow-rates (a) 10 sccm and (b) 150 sccm. The width of the low-coverage region (Δ) is shown for each case and is measured parallel to the V-groove wall.

sample into 40 wt% KOH solution held at $70\ ^\circ\text{C}$. Thermal oxidation was then employed to produce a SiO_2 passivation layer (also 120 nm in thickness) over the entire substrate. When producing contacted samples, optical lithography was used to form NiCr/Au contacts extending down to the V-groove apexes. Contacted V-grooves were formed with lengths 50 and $150\ \mu\text{m}$. Samples were then mounted inside the high vacuum chamber of the cluster deposition system.

The Sb clusters used in this work were produced in an inert gas aggregation source [16]. In this source, argon and/or helium is introduced into the source chamber to assist in the aggregation process, then a series of nozzles and differential pumping stages remove the gas, resulting in a beam of clusters which enters a high vacuum deposition chamber. The average velocity of clusters in the beam is controlled by the Ar flow-rate into the source, which was varied between 10 and 150 sccm for these experiments. For a given Ar flow-rate, the cluster deposition rate was adjusted using the temperature of the crucible and monitored with a quartz crystal film thickness monitor (FTM) mounted in line with the cluster beam. Deposition started when the sample mount was moved in front of the FTM and an electronic shutter was opened. Samples were at room temperature throughout all experiments and were mounted with their surface perpendicular to the incident cluster beam. The clusters are incident at an angle of 35° with respect to the V-groove walls ([111] planes in the underlying silicon) and at 90° to the planar surfaces between the V-grooves.

At a fixed Ar flow rate, the cluster size can be decreased by addition of He into the source chamber. At the maximum

He flow rate used here (90 sccm) this results in a 50% increase in the source pressure (at Ar flow rate 60 sccm) and, since the velocity of the gas at the exit aperture of the source chamber depends only on the pressure difference across the aperture, a modest increase in cluster velocity.

Note that whilst the velocity of the inert gas leaving the source can be calculated (given the nozzle diameter and inlet flow rate), the unknown size of the velocity slip effect² [17] means that precise calculation of the cluster velocity is impossible. We therefore prefer to quote the experimental source inlet gas flow rates when describing this work, but estimate that the average velocity of the clusters incident on the V-grooved substrates is approximately equal to the source exit gas velocity. Source exit gas velocities of 36, 41, 47 and $55\ \text{m s}^{-1}$ have been calculated for the source configuration used to produce the results shown in figures 1–5, with Ar inlet flow-rates of 30, 60, 90 and 150 sccm, respectively.

3. Results and discussion

Figure 1 shows field emission (FE) SEM images of passivated V-grooves after cluster depositions performed with Ar flow-rates of (a) 10 sccm and (b) 150 sccm. Deposition times were selected to give similar cluster densities (per unit length) in the V-grooves. It is immediately apparent that the clusters are not distributed uniformly. The clusters have a high density at the apex of the V-groove and there is a region near the top of

² Clusters are accelerated by the gas flowing through the source chamber exit nozzle but are unlikely to reach the speed of the gas flow.

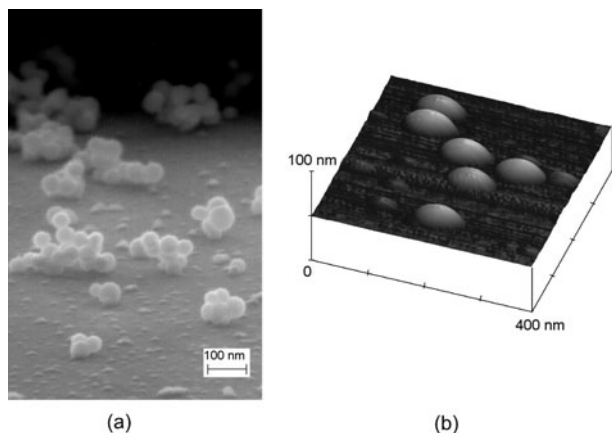


Figure 2. (a) FE-SEM image of Sb clusters on a SiO₂ surface and (b) AFM image of Bi clusters on a SiO₂ surface. The contact angle between the SiO₂ surface and the Sb clusters is approximately 120° whilst the Bi/SiO₂ contact angle is approximately 30°.

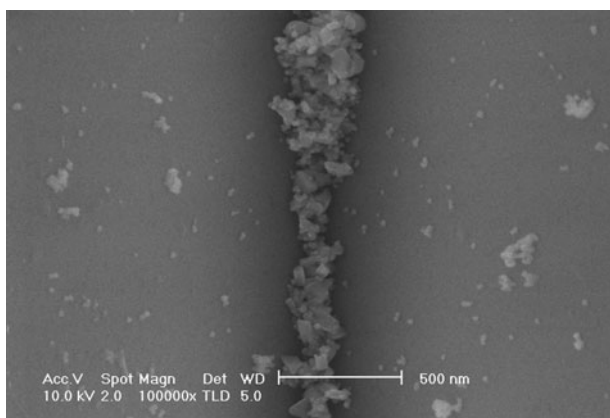


Figure 3. Sb cluster assembled wire with minimum width of less than 100 nm, formed from irregular shaped clusters at the edge of the cluster beam-spot. The source inlet Ar flow-rate was 150 sccm.

the V-groove with a low cluster density. The width of the low-coverage region is indicated in figures 1(a) and (b) and denoted Δ . In addition, the planar surfaces between V-grooves have significantly lower cluster density than found at the apex of the V-grooves and, as shown in figure 1(b), the cluster coverage on these planar surfaces and on the upper V-groove walls is almost zero at high Ar flow rates. The central result of this work is that cluster wires can be formed at the apex of the V-grooves with no possibility of parasitic conduction paths.

The average cluster diameter (~ 40 nm) is the same in figures 1(a) and (b), indicating that coalescence of clusters is not significant even in the very high coverage region at the apex of the V-groove in figure 1(b). Figure 2(a) shows a high-resolution FE-SEM image of ~ 40 nm Sb clusters on the upper part of a SiO₂-passivated V-groove which was mounted on a 25° angled stub so that the V-groove walls were almost parallel to the imaging electron beam. The majority of deposited Sb clusters are approximately spherical with high contact angles to the underlying surface. Figure 2(b) shows an AFM image of Bi clusters on SiO₂ showing that Bi clusters wet the surface to a much greater extent. (Note that FE-SEM images of Bi clusters indicate the same wetting behaviour, but it is difficult to obtain good quality high resolution images of the flatter

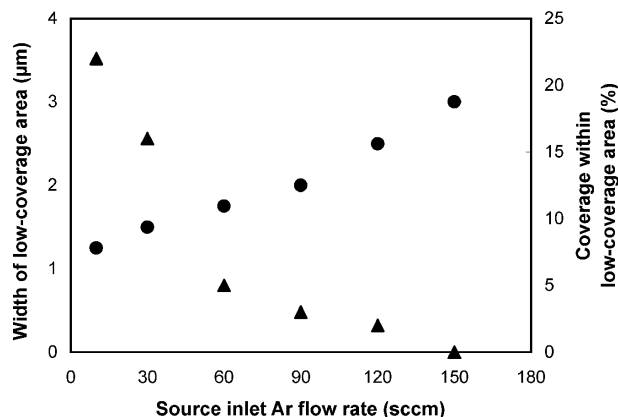


Figure 4. Width of the low-coverage region (Δ) found on the walls of 4 μm wide SiO₂ passivated Si V-grooves (\bullet) and the coverage within this region (\blacktriangle) for various Ar flow-rates.

Bi clusters.) The Sb and Bi clusters in figure 2 clearly have very different contact angles to the SiO₂ surface—as discussed further below this provides an important pointer to the cluster assembly mechanism.

Figure 3 shows an Sb cluster assembled wire with a minimum width of less than 100 nm (1/40th of the width of the V-groove) formed in a 4 μm wide V-groove and at the perimeter of the cluster beam-spot. Irregular shaped and sized (20–100 nm) Sb clusters were found around the perimeter of the cluster beam-spot³, but as shown in figure 3, these clusters assembled at the apexes of V-grooves in a similar fashion to the more commonly encountered spherical clusters.

FE-SEM images of clusters deposited on 4 μm wide V-grooves using different Ar flow-rates have been used to measure Δ and the coverage (percentage of a monolayer) within these low-coverage regions (figure 4). When clusters are deposited at low flow-rates (10–60 sccm) there is an increased density of clusters at the apex of the V-groove, but there is significant coverage on the whole of the sidewall (figure 1(a)). The clusters ‘pile up’ against each other, leading to a wire with a substantially V-shaped cross-section, suggesting that clusters have slid from the upper part of the V-groove wall. In the high-flow regime (90–150 sccm) there is almost zero coverage of clusters on the V-groove sidewalls (figure 1(b)) and no ‘pile-up’; the lower image in figure 1(b) clearly shows that the wires have a more rounded cross-section which suggests that the clusters have bounced away from the surface of the V-groove before assembling near the apex.

The low cluster coverages on the SiO₂ plateaus suggest that Sb clusters bounce off these planar surfaces. We have tested this by placing a plate with an aperture in it ~ 3 mm from the sample, so that the cluster beam passes through the aperture on the way to the sample. The significant quantities of clusters found after deposition on the side of the plate facing the sample can only be explained by clusters bouncing off the sample and back towards the plate.

A possible alternative explanation for the absence of Sb clusters on the plateaus might be that they move off the plateaus through surface diffusion [8–10, 13, 14]. However this can be discounted due to the large widths (8 μm) of the plateaus and

³ Irregular particles are expected to be spread over a larger beam spot due to lift forces. See [18].

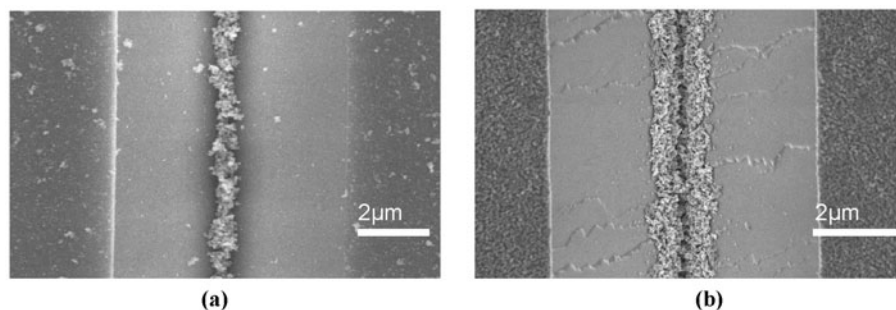


Figure 5. FE-SEM images of (a) Sb and (b) Bi cluster-assembled wires in SiO₂ passivated Si V-grooves. These wires were produced with identical source Ar flow-rates and deposition rates.

their RMS surface roughness (~ 5 nm). In addition, clusters diffusing on graphite have previously been shown to aggregate at even atomic surface steps [10]. In this work clusters do not decorate surface defects, such as ridges sometimes observed on the sides of V-grooves, and the amount of material apparent on the planar surfaces (see figure 1(b), top) is far less than that deposited. Hence diffusion of the clusters can be categorically ruled out.

Figure 5 shows Sb and Bi clusters of comparable size⁴ deposited on SiO₂ passivated V-grooves with identical Ar source inlet flow and identical deposition rate (measured using a quartz crystal FTM). In figure 5(b) the wires assembled from Bi clusters have V-shaped cross-sections (i.e. the clusters ‘slide’ and ‘pile up’ from the apex of the V-groove) whilst Sb cluster-assembled wires have rounded cross-sections (indicating that the clusters bounce rather than slide). The cluster coverage on the plateaus in figure 5(a) is less than 5% of a monolayer whilst the coverage in figure 5(b) exceeds 100% suggesting that Bi clusters stick to the plateaus much more readily than Sb clusters. Both the change in cross-section (sliding versus bouncing) and the change in plateau coverage indicate a difference in the assembly of the Bi and Sb clusters. Since the density, size and velocity of the clusters are very similar, and the substrate and deposition conditions identical, the differences in assembly must be due to the differences in the wetting of the surface by the different cluster materials. This leads us to consider the bouncing droplet model discussed below.

The existing cluster literature does not seem to provide a framework in which to understand the bouncing/sliding cluster phenomenon. A comprehensive review of the different possible outcomes of cluster deposition [19]—which include soft-landing, fragmentation, implantation and sputtering—recognizes the possibility of reflection from ‘hard’ surfaces but there appear to be no previous simulations or experiments that directly demonstrate this. Considering the large number of studies of fragmentation in the literature, the relatively small size distribution of the clusters and lack of evidence for fragmentation (figure 1) is very surprising. The large (~ 40 nm) Sb clusters which bounce in the present experiments, having high total kinetic energies (> 10 keV) but very low energies per atom (< 0.01 eV/atom), are in a distinctly different regime to those considered in previous simulations and experiments.

⁴ The average Bi and Sb cluster diameters were measured using the FE-SEM in areas of very low coverage (where little or no coalescence of the Bi clusters had taken place) and were 45 ± 5 and 40 ± 5 nm, respectively.

Simulation studies of thin film formation as a result of cluster deposition [20] have shown that different film morphologies are expected for different incident energies, but bouncing of clusters was not observed. Reference [20] shows that in the soft landing regime (< 1 eV/atom) [19], films of small clusters should be relatively lightly packed, with minimal coalescence, i.e. with open structures similar to that shown in figure 1(b).

The bouncing (nanoscale) cluster phenomenon does however appear to have many similarities with a model of bouncing (microscale) liquid droplets [21, 22] which was used in the 1950s to explain the bouncing of water droplets from leaves and other surfaces. The principle of this model is that if the kinetic energy of a rebounding droplet (E_r) is greater than the energy of attachment to the surface (E_a), i.e. if $\xi = E_r/E_a > 1$, the droplet will bounce. In this model E_r is assumed to be a fixed fraction of the kinetic energy of the incoming droplet E_i , i.e. it is assumed that a constant fraction of E_i is dissipated. Following [21] it is assumed here that $E_r/E_i = 0.50$ for all clusters. $E_a = 4\pi a^2 \gamma f(\theta)$ is the gain in surface energy associated with the droplet wetting the surface, where a is the radius of the spherical incoming droplet, γ is the surface tension of the liquid and $f(\theta)$ is a function which takes into account the change in surface energy due to the change in geometry of the droplet [22] when it wets the surface.

The observed wetting of the surface by both Bi and Sb clusters (figure 2) is evidence of a strong cluster–surface interaction, and suggests that the clusters could be treated as droplets. The known values for the surface tension⁵ and cohesive energy⁶ of Sb and Bi are very similar, suggesting that the wetting properties of the surface are crucial. Using the FE-SEM images in figure 2(a) to estimate the wetting angle (θ) for Sb clusters on SiO_x ($\theta = 120^\circ$), and following [21], figures 6 and 7 show ξ for the range of cluster sizes and velocities relevant to these studies⁷: Sb clusters ~ 40 nm in diameter are expected to bounce ($\xi > 1$) for velocities ≥ 50 m s⁻¹, which are certainly exceeded in the present experiments. Similar calculations suggest that because Bi clusters wet the surface significantly more (AFM images such as that in figure 2(b) allow an estimate $\theta \sim 30^\circ$ on SiO₂—preliminary measurements indicate that Bi also strongly wets

⁵ $\gamma(\text{Bi}) = 378$ mN m⁻¹, $\gamma(\text{Sb}) = 367$ mN m⁻¹, data from [23].

⁶ Cohesive energies are 2.75 eV/atom for Sb and 2.18 eV/atom for Bi, from [24].

⁷ Following [21] it is assumed that $E_r/E_i = 0.50$. The value of E_a is largely determined [21, 22] by $f(\theta)$, where $f(120^\circ) = 0.055$, and $f(30^\circ) = 0.75$.

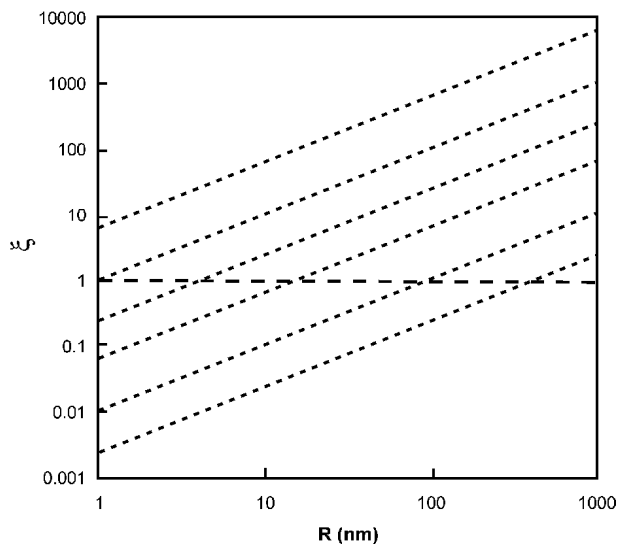


Figure 6. Ratio ξ of the kinetic energy of a reflected Sb cluster to the energy of attachment to a surface calculated (see footnote 7) as a function of cluster radius, R . $\xi > 1$ indicates that the cluster should bounce. The incident cluster velocities are 500, 200, 100, 50, 20, 10 m s^{-1} (from top to bottom).

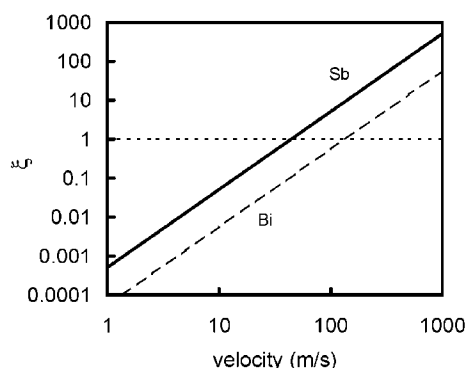


Figure 7. Ratio ξ of the kinetic energy to the attachment to a surface energy of reflected 40 nm diameter Sb and Bi clusters calculated (see footnote 7) as a function of cluster velocity. $\xi > 1$ indicates that the cluster should bounce.

SiN but that θ is slightly smaller) than Sb clusters, the incident kinetic energies need to be ~ 10 times greater for Bi clusters to bounce (i.e. for a given size Bi clusters need to travel three times faster—see figure 7). This predicted behaviour is in at least qualitative agreement with the results of figure 5 in which Bi clusters appear to be significantly ‘stickier’ than equivalent Sb clusters. Bi clusters deposited at high velocities (Ar flow rate 150 sccm) result in wire morphologies similar to Sb wires formed at low flow rates (compare figure 5(b) with 1(a)). It should be emphasized that, having discounted diffusion and since the wetting angle is the only relevant parameter which is significantly different for Bi and Sb, there is no alternative model available for the different behaviours of Sb and Bi clusters in these experiments.

The model suggests that for a given velocity, smaller clusters, having lower kinetic energies, will have a much greater probability of sticking to a surface. Figure 8 shows identical silicon dioxide passivated V-grooved substrates on which Sb clusters have been deposited with identical Ar source

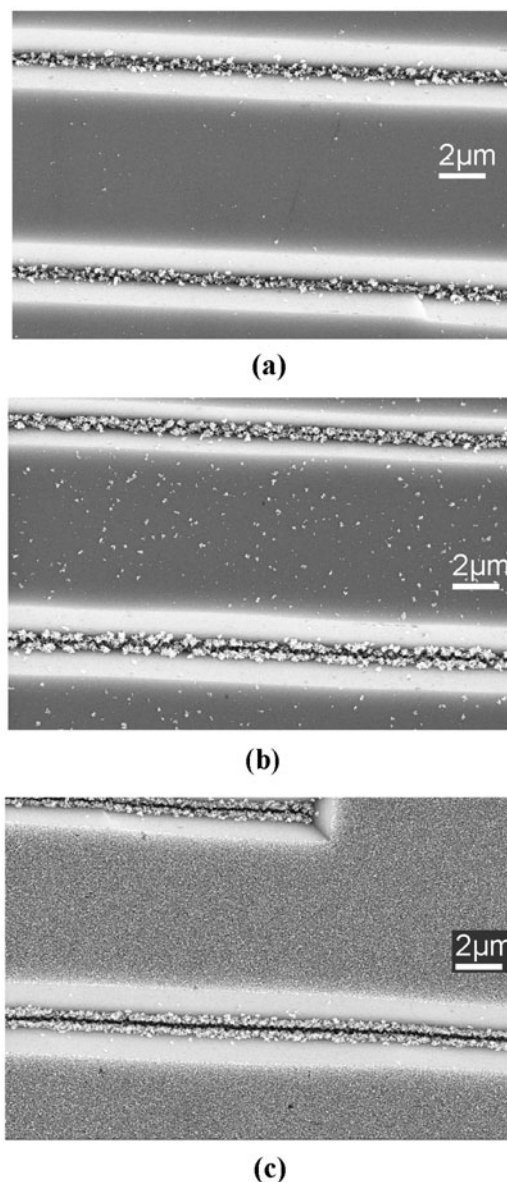


Figure 8. Cluster assembled wires produced on passivated Si V-grooved substrates from Sb clusters of average diameter (a) 40 nm (Ar/He source flow-rates—60/0 sccm), (b) 25 nm (Ar/He source flow-rates—60/30 sccm) and (c) 15 nm (Ar/He source flow-rates—60/90 sccm). These Ar/He cluster growth experiments were carried out in a new deposition system with a higher pumping speed and smaller nozzles to those used to obtain results in figures 1–5.

flow-rate, but with additional He source flow-rates which result in a decrease in the average cluster diameter: in figures 8(a)–(c), the average cluster diameters are 40, 25 and 15 nm, respectively. The key feature of figure 8 is the progression from almost zero cluster coverage on the plateaus in figure 8(a) to complete coverage in figure 8(c). Since, as discussed above, the velocity of the clusters increases slightly from (a) to (c) this progression is attributed to the different mass of the clusters (varying by a factor of $(15/40)^3 - 1/20$ from (a) to (c)) giving rise to a difference in kinetic energy of the clusters and a corresponding difference in the probability of reflection from the planar surface.

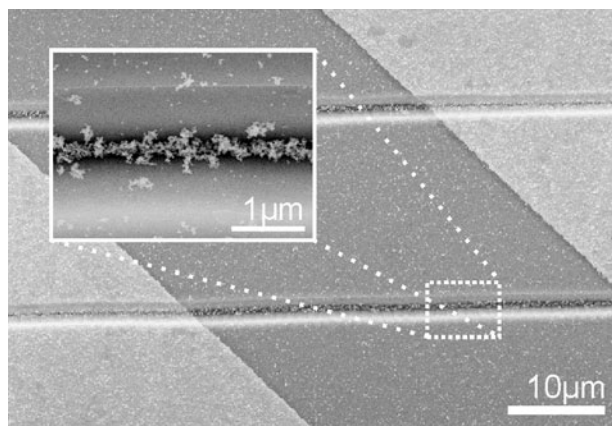


Figure 9. Contacted Sb cluster assembled wires of average width 400 nm and length 50 μm . Source inlet Ar flow-rate was 90 sccm. These wires were produced using the new deposition system as in figure 8.

A pair of contacted Sb cluster-assembled wires is shown in figure 9. A voltage (5 mV) was applied across the contacts of the V-grooves during the cluster deposition experiment and an onset of conduction for the Sb wires was observed using a picoammeter. The source flow-rate was optimized to produce wires with rounded cross-sections in the 3 μm wide V-grooves. The wires (length 50 μm) both have sub-micron widths (~ 400 nm). The resistance of this pair of parallel wires was 16 k Ω at 300 K which represents a significant improvement over our previous best results (700 k Ω) which were achieved with much wider (3 μm) wires with a V-shaped cross-section.

The cluster-assembled wires in figure 9 have resistivities $\sim 80 \times 10^{-6} \Omega \text{ cm}^{-1}$ which is much larger than the resistivity of bulk Sb ($0.4 \times 10^{-6} \Omega \text{ cm}^{-1}$) because the clusters are not fully compacted together. The conducting paths through the disordered ~ 400 nm wires in figure 9 can be considered to have effective cross-sectional areas equivalent to those of solid Sb wires with smaller diameters: a pair of cylindrical wires, each with diameter ~ 30 nm and length 50 μm , and with resistivity equal to the bulk resistivity of Sb, would have the same resistance as the cluster-assembled wires in figure 9. This indicates that current flow in the wires in figure 9 is limited by paths which may be as narrow as the diameter of a single cluster. Further work should allow us to achieve more compact, less disordered wires with still lower resistivities.

4. Summary

In summary, both contacted and uncontacted Sb cluster assembled wires have been fabricated using a templated-assembly method on SiO_2 passivated Si substrates. These wires have been fabricated with widths down to ~ 100 nm (corresponding to 1/40th of the V-groove width) and lengths up to 150 μm . Lithographically defined contacts enable the formation of the wire to be monitored and the onset of conduction to be observed. The highly selective momentum-driven assembly of the clusters at the apex of the V-grooves ensures that parasitic conduction does not occur. Similar wires have been produced using both bismuth clusters and unpassivated Si surfaces. These results will be discussed in detail elsewhere.

The assembly of the clusters at the apex of the V-groove has been shown to be due to sliding or bouncing of the clusters across the surface of the V-groove. It has also been shown that Sb clusters bounce off the planar surface between V-grooves. Comparison with results for Bi clusters, which appear significantly stickier than Sb clusters, leads to the conclusion that it is the wetting of the surface that controls the cluster assembly process. A bouncing liquid droplet model explains the main trends in the data i.e. the increased probability of bouncing for clusters that are faster, larger, or which wet the surface less.

References

- [1] Haberland H (ed) 1993 *Clusters of Atoms and Molecules: Theory, Experiment and Clusters of Atoms* (Berlin: Springer)
- [2] Meiwes-Broer K-H (ed) 2000 *Metal Clusters at Surfaces* (Berlin: Springer)
- [3] Chen W, Ahmed H and Nakazoto K 1995 *Appl. Phys. Lett.* **66** 3383
- [4] Klein D L, McEuen P L, Bowen Katari J E, Roth R E and Paul Alivisatos A 1996 *Appl. Phys. Lett.* **68** 2574
- [5] Schmelzer J Jr, Brown S A, Wurl A, Hyslop M and Blaikie R J 2002 *Phys. Rev. Lett.* **88** 226802
- [6] Bezryadin A, Dekker C and Schmid G 1997 *Appl. Phys. Lett.* **71** 1273
- [7] Thelander C, Magnusson M H, Deppert K, Samuelson L, Rugaard Poulsen P, Nygard J and Borggreen J 2001 *J. Appl. Phys. Lett.* **79** 2106
- [8] Kaiser B, Stegemann B, Kaukel H and Rademann K 2002 *Surf. Sci. Lett.* **496** L18
- [9] Howells A R, Hung L, Chottiner G S and Scherson D A 2002 *Solid State Ion.* **150** 53
- [10] Francis G M, Kuipers L, Cleaver J R A and Palmer R E 1996 *J. Appl. Phys.* **79** 2942
- [11] Brechignac C, Cahuzac Ph, Carlier F, Colliex C, Leroux J, Masson A, Yoon B and Landman U 2002 *Phys. Rev. Lett.* **88** 196103
- [12] Favier F, Walter E C, Zach M P, Benter T and Penner R M 2001 *Science* **293** 2227
- [13] Bardotti L, Prevel B, Jensen P, Treilleux M, Melinon P, Perez A, Gierak J, Faini G and Maily D 2002 *Appl. Surf. Sci.* **191** 205
- [14] Liu J, Barnard J C, Seeger K and Palmer R E 1998 *Appl. Phys. Lett.* **73** 2030
- [15] Parker A J, Childs P A, Palmer R E and Brust M 1999 *Appl. Phys. Lett.* **74** 2833
- [16] deHeer W A 1993 *Rev. Mod. Phys.* **65** 611
- [17] Hall B 1991 *PhD Thesis* EPFL, Lausanne, Switzerland
- [18] Liu P, Ziemann P J, Kittelson D B and McMurry P H 1995 *Aerosol Sci. Technol.* **22** 293
- [19] Harbich W 2000 *Metal Clusters at Surfaces* ed K-H Meiwes-Broer (Berlin: Springer) chapter 4
- [20] Haberland H, Insepov Z and Moseler M 1995 *Phys. Rev. B* **51** 11061
See also Moseler M, Rattunde O, Nordick J and Haberland H 1998 *Comput. Mater. Sci.* **10** 452
- [21] Davies J T and Rideal E K 1961 *Interfacial Phenomena* (New York: Academic) p 441
- [22] Hartley G S and Brunskill R T 1958 *Surface Phenomena in Chemistry and Biology* ed J F Danielli, K G A Pankhurst and A C Riddiford (London: Pergamon) p 214
- [23] Smithells C J 1976 *Metals Reference Book* 5th edn (Woburn, MA: Butterworth-Heinemann)
- [24] Kittel C 1996 *Introduction to Solid State Physics* 7th edn (New York: Wiley) p 57